JACS
JOURNAL OF THE AMERICAN CHEMICAL SOCIETY

Communication

pubs.acs.org/JACS

Structurally Ordered Nanowire Formation from Co-Assembly of DNA Origami and Collagen-Mimetic Peptides

Tao Jiang,[†,⊥,#] Travis A. Meyer,[‡,#] Charles Modlin,[†] Xiaobing Zuo,[§] Vincent P. Conticello,[*,†] and Yonggang Ke[*,‡]

[†]Department of Chemistry, Emory University, Atlanta, Georgia 30322, United States

[‡]Wallace H. Coulter Department of Biomedical Engineering, Georgia Institute of Technology and Emory University, Atlanta, Georgia 30322, United States

[§]X-ray Science Division, Argonne National Laboratory, Argonne, Illinois 60439, United States

Supporting Information

ABSTRACT: We describe the co-assembly of two different building units: collagen-mimetic peptides and DNA origami. Two peptides **CP**$^{++}$ and **sCP**$^{++}$ are designed with a sequence comprising a central block (Pro-Hyp-Gly) and two positively charged domains (Pro-Arg-Gly) at both N- and C-termini. Co-assembly of peptides and DNA origami two-layer (**TL**) nanosheets affords the formation of one-dimensional nanowires with repeating periodicity of ∼10 nm. Structural analyses suggest a face-to-face stacking of DNA nanosheets with peptides aligned perpendicularly to the sheet surfaces. We demonstrate the potential of selective peptide-DNA association between face-to-face and edge-to-edge packing by tailoring the size of DNA nanostructures. This study presents an attractive strategy to create hybrid biomolecular assemblies from peptide- and DNA-based building blocks that takes advantage of the intrinsic chemical and physical properties of the respective components to encode structural and, potentially, functional complexity within readily accessible biomimetic materials.

Recent years have witnessed substantial advancement in molecular self-assembly with programmable biomolecules.[1] One of the ultimate goals is to rationally design molecular structures that rival the complexity and functionality of naturally occurring biomolecular assemblies. Success in this endeavor critically relies on the development of new strategies for the self-assembly of hybrid structures that consist of multiple types of biomolecules. Biology has demonstrated that co-assembly of different structural units can lead to structurally complex supramolecular assemblies that display exquisitely tailored function. The assembly of infectious tobacco mosaic virus from self-association from self-association of coat proteins on an RNA template represents a notable example (Figure 1a).[2] These native nucleoprotein assemblies have inspired efforts to create synthetic protein-DNA biomaterials that could hypothetically recapitulate the structural and functional complexity of viruses. Several approaches have been described that employ different mechanisms to control the protein-DNA interface, which include electrostatic charge complementation,[3] covalent conjugation,[4] and sequence-specific molecular recognition.[5]

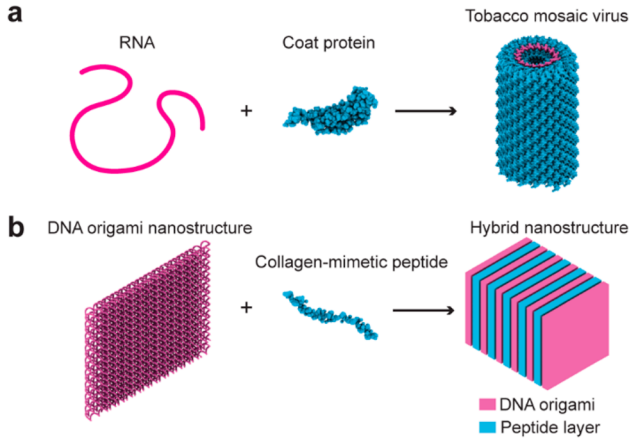

Figure 1. Concept of nanostructures assembled from DNA origami and peptide. (a) Tobacco mosaic virus assembled from coat protein and template RNA. (b) A DNA-origami-peptide nanostructure assembled from DNA-origami nanostructures and collagen-like peptide.

Herein, we demonstrate that DNA nanotechnology, which has exhibited great capacity for the rational design of complex structures across multiple length-scales[6] and holds promise for engineering hybrid biomaterials,[7] can be employed to enable co-assembly of larger ordered peptide-DNA nanostructures (Figure 1b).

In contrast to both naturally occurring nucleic-acid-protein co-assemblies and previous human-made nucleic-acid-peptide co-assembly, in which the nucleic acids generally serve as assembly templates without forming complex structures, our approach allows us to use pre-assembled, rationally designed DNA nanostructures to produce more structurally sophisticated peptide-DNA hybrid assemblies. We believe that our study will provide new information for the design and construction of peptide-DNA co-assemblies using tailored DNA nanostructures that will ultimately promote greater control over the structural and functional complexity of artificial hybrid structures.

Previously, we described a peptide **CP**$^{+}$ that self-assembled into nanoscale sheets.[8] It has a sequential triblock architecture

Received: August 7, 2017
Published: September 26, 2017

DOI: 10.1021/jacs.7b08087
J. Am. Chem. Soc. XXXX, XXX, XXX−XXX

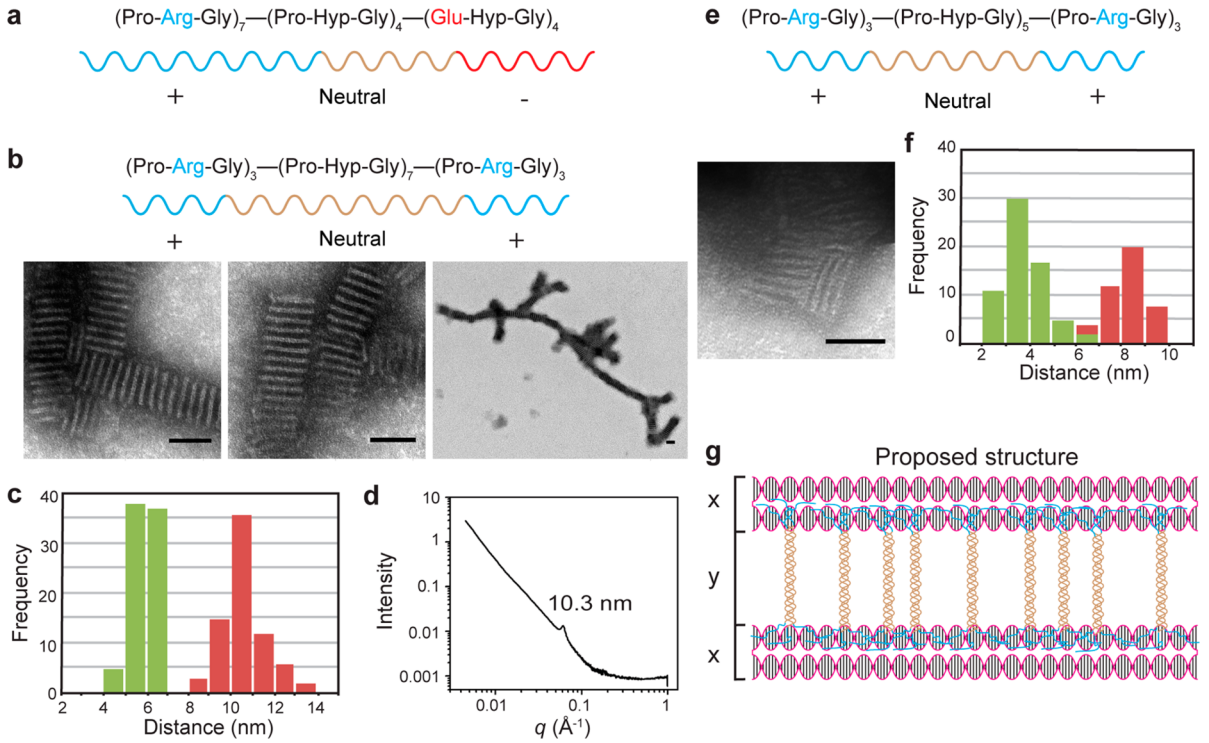

Figure 2. Nanostructures from **TL** nanosheets and collagen-like peptides. (a) Sequence of **CP**$^{+}$ peptide. (b) Sequence of **CP**$^{++}$ peptide (top) and TEM images of nanowires (bottom) assembled with **TL** and **CP**$^{++}$. (c) Histograms of the distances of **TL**-layer plus **CP**$^{++}$ peptide-layer (red, $x + y$ in (g)), and the distances of **CP**$^{++}$ peptide-layer (green, y in (g)). (d) SAXS/WAXS profile for **CP**$^{++}$-**TL** nanowires. (e) Sequence of **sCP**$^{++}$ peptide (top) and TEM images of nanowires (bottom) assembled with **TL** nanosheets and **sCP**$^{++}$. (f) Histograms of the distances of **TL**-layer plus **sCP**$^{++}$ peptide-layer (red, $x + y$ in (g)), and the distances of **sCP**$^{++}$ peptide-layer (green, y in (g)). (g) Proposed co-assembly structure. Scale bars, 50 nm.

comprising positively, neutral, and negatively charged (Xaa-Yaa-Gly) triads[9] (Figure 2a) that self-associated into collagen-like triple helices. Electrostatic attractions between oppositely charged residues on adjacent peptides[9,10] drove the assembly of the triple helices into peptide sheets. The greater length of the positively charged (Pro-Arg-Gly) domain, versus the negatively charged (Glu-Hyp-Gly) domain, ensured that the extra (Pro-Arg-Gly) triads protruded from sheet surfaces.[8] We hypothesized that those arginine-rich overhangs might be recruited for interacting with negatively charged DNA-based materials. We observed that two-layer (**TL**) DNA origami[6c] nanosheets (Figure S1; dimension ~50 nm × 50 nm × 5 nm, measured by TEM) could deposit onto the surface of pre-assembled **CP**$^{+}$ sheets (Figure S2), although the arrangement of the **TL** nanosheets on the **CP**$^{+}$ nanosheets was sporadic and not ordered.

We proposed that a new design with weakened attraction between triple helices might allow the **TL** nanosheets to assemble into more ordered structures in the presence of the peptide (Figure 1b). Two new collagen-mimic peptides **CP**$^{++}$ and **sCP**$^{++}$ were designed and synthesized to include three positively charged (Pro-Arg-Gly) triads in both the N- and C-blocks (Figure 2b,e, top). Despite the shorter central core of the **sCP**$^{++}$ (5 (Pro-Hyp-Gly) triad repeats, compared to the 7 repeats for **CP**$^{++}$), the circular dichroism (CD) spectropolarimetry of both **CP**$^{++}$ and **sCP**$^{++}$ in Tris buffer (5 mM, pH 8.0) displayed a characteristic signature of collagen-like triple helix, comprising a maximum peak at 224 nm and a minimum peak at 197 nm (Figure S3a). Thermal denaturation experiments indicated melting transition temperatures (T_m) of 63 and 52 °C for **CP**$^{++}$ and **sCP**$^{++}$ (Figure S3b). The decrease in T_m value observed for **sCP**$^{++}$ versus **CP**$^{++}$ can be attributed to the shorter central core having fewer canonical (Pro-Hyp-Gly) triads in peptide **sCP**$^{++}$.[9b] Compared to similar sequences of (Pro-Hyp-Gly)$_7$ (T_m = 41 °C),[11] **CP**$^{++}$ afforded more stable triple helices. Indeed, the (Pro-Arg-Gly) triad sequence in host-guest systems of collagen-mimetic peptides showed a comparable thermostability to the canonical triad (Pro-Hyp-Gly).[12] However, the electronic repulsion between arginines in adjacent helices prevented the triple helices of both peptides from self-assembling to higher-order structures, as has been observed previously for charge complementary collagen-mimetic peptide sequences.[8,9]

TEM investigation demonstrated that co-assembly of **CP**$^{++}$ and **TL** nanosheets (molar ratio of **CP**$^{++}$:**TL** = 1600:1 and **TL** at 20 nM) led to the formation of one-dimensional (1D) banded nanowires (Figure 2b). The width of nanowires was measured to be 47 ± 3 nm, which is close to the dimension of **TL** cross section (~50 nm × 50 nm) (Figure S1). A high peptide/**TL** sheet molar ratio (at least 1600:1) was required to maintain stable co-assembly. With a peptide concentration at 32 μM and peptide-to-DNA sheet ratio at least 1600:1, the axial length of the nanowires depended on the amount of **TL** nanosheets. With lower concentrations of **TL** nanosheets (0.35 nM), shorter assemblies were observed (Figure S4). Within nanowires, thickness of light bands (4.8 ± 0.7 nm) matched the thickness of **TL** nanosheets. The spacing between adjacent light bands (dark region in the TEM images) was measured to be 5.9 ± 0.6 nm (Figure 2c), which is on the order of the theoretical length of the central block of **CP**$^{++}$ triple helix (6.0 nm, 0.286 nm rise/residue[13] × 21 residues). Similar 1D nanostructures were observed from **sCP**$^{++}$-**TL** co-assembly incubated at 4 °C

DOI: 10.1021/jacs.7b08087
J. Am. Chem. Soc. XXXX, XXX, XXX−XXX

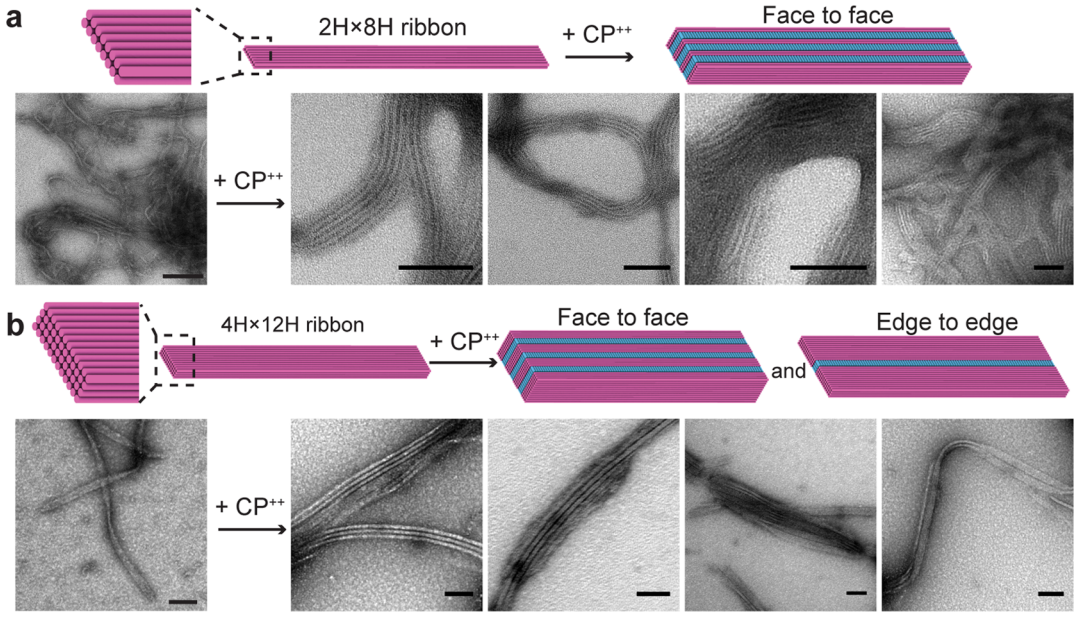

Figure 3. Models and representative TEM images of DNA ribbons and nanostructures co-assembled from ribbons and **CP**$^{++}$ peptide. (a) **2H × 8H** ribbons (left); face-to-face assembly of **2H × 8H** ribbons and **CP**$^{++}$ (right). (b) **4H × 12H** ribbons (left); face-to-face and edge-to-edge assembly of **4H × 12H** ribbons and **CP**$^{++}$ (right). Scale bars, 100 nm.

(Figure 2e, bottom), but with shorter interband distance (3.8 ± 0.9 nm) (Figure 2f), which is on the order of the theoretical length of the central block of **sCP**$^{++}$ triple helix (4.3 nm, 0.286 nm rise/residue ×15 residues). However, the **sCP**$^{++}$**-TL** co-assembly generated nanowires of noticeably shorter length (46 ± 19 nm) compared to those observed for **CP**$^{++}$**-TL** (133 ± 92 nm), presumably due to the reduced thermal stability of the **sCP**$^{++}$ triple helix (Figure S5). Significant aggregation occurred between nanowires, given the presence of much more positively charged peptides and negatively charged **TL** sheets in nanowires (Figure S4). The aggregation may be mitigated by designing new **TL** nanosheets carrying neutral change on the edges.

The **CP**$^{++}$**-TL** nanowires proved more robust toward structural analysis and were further investigated using synchrotron SAXS/WAXS (Figures 2d and S6). A Bragg reflection was observed in the scattering profile, indicating a high order of internal structure. The peak at q = 0.061 ± 0.004 Å^{-1} corresponds to a d-spacing of 10.3 ± 0.7 nm (Figures 2d and S6). We assigned it to the periodic center-to-center distance of adjacent light bands (equals to $x + y$ in Figure 2g), which agrees with the axial spacing 10.6 ± 1.0 nm derived from TEM measurements (Figure 2c). Scherrer analysis[14] of the diffraction peak width provided an average length of 109 nm for the nanowires if we assumed that the peak broadening was mainly caused by the finite nanowires length (Figure S6). A structural model was proposed that **TL** nanosheets (light band in TEM) are separated by peptides (dark band in TEM) and adopt a face-to-face stacking configuration (Figures 1b and 2g). Since the intersheet distances corresponded to the length of the peptides' central blocks, rather than the total length of peptides, the peptide helices likely aligned perpendicularly to the surface of the **TL** nanosheets, with the positively charged, nonordered $(Pro\text{-}Arg\text{-}Gly)_3$ domains associating with the negatively charged surface of **TL** nanosheets (Figure 2g). Additionally, hydrogen bonds could also form between the guanidinium group of arginine and the phosphate backbone or nucleobases of the nucleic acids.[15]

Interestingly, the **TL** nanosheets did not stack edge-by-edge (5 nm in thickness), suggesting that TL's edges could not provide a thermodynamically stable interaction with the **CP**$^{++}$ or **sCP**$^{++}$ (at extended state, the $(Pro\text{-}Arg\text{-}Gly)_3$ domain has a radius of 3.0 nm (0.33 nm contour length/residue[16] × 9 residues)). We designed a DNA-brick[6b] **2H × 8H** (cross section 5 nm × 20 nm) nanoribbon and a **4H × 12H** (cross section 10 nm × 30 nm) nanoribbon to further verify this observation and demonstrate that the phenomenon can be used to regulate the peptide-DNA co-assembly. The **2H × 8H** nanoribbon had the same thickness as **TL** nanosheet, while the **4H × 12H** nanoribbon was twice as thick as **TL** nanosheet. Both nanoribbons assembled into two-dimensional (2D) arrays, in the presence of **CP**$^{++}$ (Figure 3). Nonetheless, similar to the **TL** nanosheet, **2H × 8H** ribbons assembled via **CP**$^{++}$ interaction only with the large faces (8H) (Figure 3a), while **4H × 12H** ribbons assembled via **CP**$^{++}$ interaction with both the large face (12H) and thin edge (4H) (Figure 3b), in agreement with the co-assembly results of **CP**$^{++}$ and **TL** nanosheets. Notably, extensive edge-to-edge stacking was not observed by using ribbons compared to the use of 2D nanosheet. It is presumably due to the self-twisting property of such long structures that hindered the perfect alignment between adjacent ribbons (Figure 3a left, b left). Moreover, most co-assemblies using 4Hx12H ribbons adopted both face-to-face and edge-to-edge stacking within same structures.

Significant research effort is being directed currently toward the creation of hybrid biomaterials containing a combination of peptide/protein and nucleic acid components.[3−5,17] Here, we report a facile approach to co-assemble 2D DNA nanostructures and collagen-mimetic peptides into 1D hybrid materials. With DNA nanosheets, the peptides directed a face-to-face stacking of DNA nanosheets and formed nanowires. The separations between DNA nanosheets could be controlled through the length of the central block in peptide triple helices.

DOI: 10.1021/jacs.7b08087
J. Am. Chem. Soc. XXXX, XXX, XXX−XXX

We attribute the periodic structure in co-assemblies to the alignment of peptide helices, which we propose is perpendicular to the faces of DNA nanosheets. Moreover, we showed that patterns of peptide-DNA interactions could be modulated by tailoring the design of DNA nanostructures. These types of hybrid biomaterials may have an advantage for the creation of functional devices in that the distinct structures and chemical properties of the two classes of biomolecules could be combined potentially in a synergistic manner.

■ ASSOCIATED CONTENT

Supporting Information

The Supporting Information is available free of charge on the ACS Publications website at DOI: 10.1021/jacs.7b08087.

Experimental details, DNA sequences, and characterization of peptide-DNA nanostructures (PDF)

■ AUTHOR INFORMATION

Corresponding Authors

*vcontic@emory.edu

*yonggang.ke@emory.edu

ORCID

Yonggang Ke: 0000-0003-1673-2153

Present Address

⊥Department of Materials Science and Engineering, Department of Chemistry, University of California, Berkeley, Berkeley, California 94720, United States

Author Contributions

#These authors contributed equally to this work.

Notes

The authors declare no competing financial interest.

■ ACKNOWLEDGMENTS

Y.K. acknowledges financial support from NSF grant DMR-1654485. V.P.C. acknowledges financial support from NSF grant CHE-1412580. This research used resources of the Advanced Photon Source, a U.S. Department of Energy (DOE) Office of Science User Facility operated for the DOE Office of Science by Argonne National Laboratory under contract no. DE-AC02-06CH11357. The EM data described here was gathered on the Hitachi HT7700 120kV TEM supported by the Atlanta Clinical and Translational Science Institute (ACTSI) award UL1TR000454.

■ REFERENCES

(1) (a) Woolfson, D. N.; Bartlett, G. J.; Burton, A. J.; Heal, J. W.; Niitsu, A.; Thomson, A. R.; Wood, C. W. *Curr. Opin. Struct. Biol.* **2015**, *33*, 16−26. (b) Jones, M. R.; Seeman, N. C.; Mirkin, C. A. *Science* **2015**, *347*, 1260901.

(2) Stubbs, G.; Warren, S.; Holmes, K. *Nature* **1977**, *267*, 216−221.

(3) (a) Ni, R.; Chau, Y. *Angew. Chem., Int. Ed.* **2017**, *56*, 9356−9360. (b) Noble, J. E.; De Santis, E.; Ravi, J.; Lamarre, B.; Castelletto, V.; Mantell, J.; Ray, S.; Ryadnov, M. G. *J. Am. Chem. Soc.* **2016**, *138*, 12202−12210. (c) Hernandez-Garcia, A.; Kraft, D. J.; Janssen, A. F. J.; Bomans, P. H. H.; Sommerdijk, N. A. J. M.; Thies-Weesie, D. M. E.; Favretto, M. E.; Brock, R.; de Wolf, F. A.; Werten, M. W. T.; van der Schoot, P.; Stuart, M. C.; de Vries, R. *Nat. Nanotechnol.* **2014**, *9*, 698−702. (d) Ruff, Y.; Moyer, T.; Newcomb, C. J.; Demeler, B.; Stupp, S. I. *J. Am. Chem. Soc.* **2013**, *135*, 6211−6219. (e) de la Escosura, A.; Janssen, P. G. A.; Schenning, A. P. H. J.; Nolte, R. J. M.; Cornelissen, J. J. L. M. *Angew. Chem., Int. Ed.* **2010**, *49*, 5335−5338.

(4) Kye, M.; Lim, Y. B. *Angew. Chem., Int. Ed.* **2016**, *55*, 12003−12007.

(5) (a) Praetorius, F.; Dietz, H. *Science* **2017**, *355*, eaam5488. (b) Mou, Y.; Yu, J. Y.; Wannier, T. M.; Guo, C. L.; Mayo, S. L. *Nature* **2015**, *525*, 230−233.

(6) (a) Veneziano, R.; Ratanalert, S.; Zhang, K. M.; Zhang, F.; Yan, H.; Chiu, W.; Bathe, M. *Science* **2016**, *352*, 1534. (b) Ke, Y. G.; Ong, L. L.; Shih, W. M.; Yin, P. *Science* **2012**, *338*, 1177−1183. (c) Rothemund, P. W. K. *Nature* **2006**, *440*, 297−302. (d) Winfree, E.; Liu, F. R.; Wenzler, L. A.; Seeman, N. C. *Nature* **1998**, *394*, 539−544.

(7) (a) Udomprasert, A.; Bongiovanni, M. N.; Sha, R.; Sherman, W. B.; Wang, T.; Arora, P. S.; Canary, J. W.; Gras, S. L.; Seeman, N. C. *Nat. Nanotechnol.* **2014**, *9*, 537−541. (b) Yan, H.; Park, S. H.; Finkelstein, G.; Reif, J. H.; LaBean, T. H. *Science* **2003**, *301*, 1882−1884. (c) Niemeyer, C. M.; Sano, T.; Smith, C. L.; Cantor, C. R. *Nucleic Acids Res.* **1994**, *22*, 5530−5539.

(8) Jiang, T.; Vail, O. A.; Jiang, Z. G.; Zuo, X. B.; Conticello, V. P. *J. Am. Chem. Soc.* **2015**, *137*, 7793−7802.

(9) (a) Jiang, T.; Xu, C. F.; Zuo, X. B.; Conticello, V. P. *Angew. Chem., Int. Ed.* **2014**, *53*, 8367−8371. (b) Jiang, T.; Xu, C. F.; Liu, Y.; Liu, Z.; Wall, J. S.; Zuo, X. B.; Lian, T. Q.; Salaita, K.; Ni, C. Y.; Pochan, D.; Conticello, V. P. *J. Am. Chem. Soc.* **2014**, *136*, 4300−4308. (c) O'Leary, L. E. R.; Fallas, J. A.; Bakota, E. L.; Kang, M. K.; Hartgerink, J. D. *Nat. Chem.* **2011**, *3*, 821−828.

(10) (a) Parmar, A. S.; James, J. K.; Grisham, D. R.; Pike, D. H.; Nanda, V. *J. Am. Chem. Soc.* **2016**, *138*, 4362−4367. (b) Tanrikulu, I. C.; Forticaux, A.; Jin, S.; Raines, R. T. *Nat. Chem.* **2016**, *8*, 1008−1014.

(11) Rubert Pérez, C. M.; Rank, L. A.; Chmielewski, J. *Chem. Commun.* **2014**, *50*, 8174−8176.

(12) Persikov, A. V.; Ramshaw, J. A. M.; Brodsky, B. *J. Biol. Chem.* **2005**, *280*, 19343−19349.

(13) Okuyama, K.; Miyama, K.; Mizuno, K.; Bächinger, H. P. *Biopolymers* **2012**, *97*, 607−616.

(14) Cullity, B. D.; Stock, S. R. *Elements of X-Ray Diffraction*; 3rd ed.; Prentice Hall: Upper Saddle River, NJ, 2001.

(15) Rohs, R.; West, S. M.; Sosinsky, A.; Liu, P.; Mann, R. S.; Honig, B. *Nature* **2009**, *461*, 1248−1253.

(16) Terao, K.; Mizuno, K.; Murashima, M.; Kita, Y.; Hongo, C.; Okuyama, K.; Norisuye, T.; Bächinger, H. P. *Macromolecules* **2008**, *41*, 7203−7210.

(17) Zhang, C. Q.; Zhan, T. B.; Jin, S. B.; Xue, X. D.; Yang, X. L.; Gong, N. Q.; Zhang, J. C.; Wang, P. C.; Tian, J. H.; Xing, J. F.; Liang, X. J. *ACS Appl. Mater. Interfaces* **2017**, *9*, 4425−4432.

DOI: 10.1021/jacs.7b08087
J. Am. Chem. Soc. XXXX, XXX, XXX−XXX